# VENTILATION SYSTEM DESIGN FOR A ROADWAY TUNNEL IN ACAPULCO, MÉXICO

Alejandro Rodríguez, Arturo Palacio, Andrés Aramayo
Instituto de Ingeniería de la UNAM
ap. post. 70-472, Coyoacan, México D.F., 04510

Date: July 1998
Computer and operating system used: HP/750, HP-UX 9.05
PHOENICS version 2.1

*Abstract*

There are several industrial methods for tunnel ventilation system design. In particular, for tunnels where axial flow fans are applicable, there are specialized computer programs that calculate the various pressure drops that consider wall friction and local losses due to signs and appurtenances, and considering vehicle emission factors based on up-hill or down-hill conditions, determine the number of axial fans that satisfy the tunnel ventilation requirements. Based on drag coefficient factors, they can also estimate the effect of favourable or adverse traffic lane direction.

Given the magnitude of the capital investment in the electromechanical installation for a new 3 km tunnel that would reduce access time to the port city of Acapulco, Mexico, from 1 h to 10 minutes, a PHOENICS simulation was performed that would optimize the number and distribution of axial flow fans.

The model was set up for the prototype dimensions of the Acapulco Tunnel and simulations were performed based on maximum CO concentration criterion, considering three lane traffic with two adverse and one favourable with the axial fan flow. Based on the analysis of results, the number of fans implemented in the operating tunnel was significantly reduced from a design derived from the aforementioned computer programs.

*Objective of work*

The main objective of the work presented was to determine the number and arrangement of jet fans to be installed in the Acapulco Tunnel that will ensure an air quality that meets international standards for vehicle occupants.

During the design stage of the ventilation system for this tunnel, questions arose as whether to apply a cement coating finish on the walls to reduce the surface roughness, and whether the required number of fans as specified by the specialised programs exceeded the design constraints.

*Description of phenomenon simulated*

The new schemes for tunnel ventilation are more suited for the longitudinal systems since they are generally shorter or have been built as twin-tubes for one-way traffic, where the piston effect of the traffic will combine with the fans to produce the required ventilation flow. Longitudinal ventilation offers a relatively simple and cheap method for ventilating road tunnels. Further, this arrangement offers the best response to the most feared of tunnel incidents that is a fire. A semi or fully transverse system offers the most positive method of smoke removal from a tunnel. In a longitudinal system the smoke must be removed along the traffic space and therefore operational procedures for the tunnel must be prepared to ensure maximum safety for users.

Generally, two-way fans should be installed to enable them to blow in the direction of the major traffic flow. Where the adverse wind velocity pressure can be so high as to negate the vehicle and fan induced thrusts in the direction of the dominant traffic, then it becomes necessary to increase the power of the fans or to install reversible fans. An automatic control system responding to the wind becomes necessary.

Wind represents the great-unknown quantity in most longitudinal ventilation system designs. Opposing winds will slow down the tunnel airflow. In any design sufficient fans are to be provided to create an adequate air supply on all but those occasions when traffic congestion coincides with strong adverse winds. Measurement of the velocity and direction for the wind exterior to the tunnel would be ideal, but unless there is sufficient data accumulated to derive the effects on the tunnel air-flow, this approach will be frustrated by local turbulence.

Current design practice allows a maximum CO concentration of 150 ppm as recommended by the PIARC (Permanent International Association of Road Congresses) for flowing traffic. It should be remarked that heavy smokers are exposed to much higher concentrations; the air exhaled is around 185 ppm of CO, concentration in the smoke inhaled is even higher. This is the most significant parameter for the safety of vehicle passengers. The other design parameter is visibility that is mainly affected by particle emissions from diesel engines, but this is not a significant problem in longitudinal ventilation tunnels as they are limited in the maximum tunnel length.

Qualitative

The induced flow in a tunnel by the stream of a jet fan is a consequence of the momentum exchange of the high speed jet with the air flow in the tunnel section in the proximity of the fan, in a similar fashion as it is effected in a jet-pump. Two important exchange zones can be distinguished: in the output region of the fan where the proximity of the tunnel ceiling allows for a high momentum sink due to friction, and downstream between fans where most of the mixing takes place. Ideally the velocity deceleration increases the static pressure in the tunnel which in turn drives the flow against the friction pressure loss. However, there are two factors that

decrease the efficiency of this momentum transfer process: turbulent dissipation in the jet mixing process and flow separation zones in the vicinity of the fan. To quantify these effects proper grid resolution is required in the ‘near field‘ of the fan inlet and outlet.

Experimental data regarding the influence of wall proximity on fan jet to tunnel air momentum exchange is limited, but there is an attachment of the jet to this boundary that tends to increase the friction losses given the high speed of the jet. Advantages can therefore be found in an optimum jet axis inclination to the horizontal direction.

Another source of momentum source/sink is the ’piston effect’ induced by the vehicle drag. Given the two-way nature of traffic that is to be represented, these sources were modelled by a ‘moving wall’ that causes positive or adverse shear on the airflow. Although this is not a physically accurate representation, the overall effect on the power requirements and the pollutant concentration distribution would seem adequate.

## Mathematical

The three dimensional model is based on the solution to the conservation equations as afforded by PHOENICS. Since carbon monoxide concentration *C* in the tunnel is the basis for a satisfactory design, a species conservation equation is also solved to calculate its convective and dispersive transport within the tunnel. Buoyancy effects due to temperature differences are not considered, and the energy equation is therefore not solved.

Considering a steady state, the conservation equations that consider the Boussinesq approximation for turbulent flows are:

$$\frac{\partial U_i}{\partial x_i} = 0 \qquad (1)$$

$$U_j \frac{\partial U_i}{\partial x_j} = -\frac{1}{\rho}\frac{\partial p}{\partial x_i} + \frac{\mu_t}{\rho}\nabla^2 U_i + S_{U_i} \qquad (2)$$

$$U_j \frac{\partial C}{\partial x_j} = \frac{\mu_t}{\rho \sigma_C}\nabla^2 C + S_C \qquad (3)$$

where the indices are *i,j* = 1,2,3; i.e. $(x_1,x_2,x_3) = (x,y,z)$, $(U_1,U_2,U_3) = (u,v,w)$, and the source terms are represented by $S_\phi$ , ($\phi = U_i , C$ ).

The $k$ - $\varepsilon$ turbulence model is implemented, which solves two additional transport equations for the turbulent kinetic energy and the dissipation rate with the corresponding turbulence production and dissipation sources. Cell values of $k$ and $\varepsilon$ are then used to calculate the turbulent viscosity that is used in the momentum equation:

$$\nu_t = \frac{\mu_t}{\rho} = c_\mu \frac{k^2}{\varepsilon} \qquad (4)$$

where $c_\mu$ has a constant value of 0.09; and the Schmidt number for the concentration of carbon monoxide *CO* is $\sigma_c = 1$.

Wall functions for the logarithmic velocity profile are used in all solid surfaces of the tunnel boundaries, where it is assumed that turbulence is in local equilibrium. Tunnel inlet and outlet boundary conditions are a prescribed reference pressure that is the barometric pressure (i.e. zero gage pressure). A local loss of one half the calculated dynamic pressure at the inlet is also prescribed.

The jet fans are simulated as fixed momentum sources with a prescribed design velocity value at its outlet, while solid boundaries are specified for the fan casing. Vehicle drag as a source of sink of momentum is depicted as two horizontal and two vertical moving plates for each of the three traffic lanes that have a fixed velocity of 60 km/h. Regarding traffic direction, the most adverse case is considered where in two lanes traffic direction is against the air flow and one lane is in the air flow direction induced by the jet fans.

For carbon monoxide (CO) concentration, it is assumed that the air at the inlet has zero concentration and zero gradient at the outlet. Vehicle emissions within the tunnel is represented as a line source of 5.5 ppm/($m^3$s) per lane [Baugh *et al* (1987)], which corresponds to the design vehicular density of 1,381 pv/h (pv := passenger vehicle) per lane with an emission factor of $f_{CO}$ = 1 $m^3$/(h.pv). It should be remarked that the U.S. emission factor standard for 1989 was 0.6 $m^3$/(h.pv) and 2.1 $m^3$/(h.pv) in 1967. Preliminary calculations show that 10 air volume changes per hour would allow sufficient dilution of the CO gas so that the maximum concentration would be 150 ppm. This is a flow rate of 716 $m^3$/s. Considering the tunnel length and cross section area, the specific flow rate is 243 $m^3$/(s.km), and the average air velocity is 8.2 m/s.

To obtain this airflow, the number of jet-fans and their arrangement within the tunnel was investigated. The 45 kW rating jet-fans have a thrust of 2.86 kN considering an air density of 1.19 $kg_a/m^3$, a jet area at the exit of 2.084 $m^2$, and an exit velocity of 34 m/s. The supplier of the fans had proposed that from 35 to 40 jet-fans were required to guarantee sufficient dilution of CO emissions, but preliminary calculations with the design values showed that these numbers were over rated. Two different arrangements of 21 or 24 jet-fans were therefore numerically simulated. The fans were distributed along the tunnel in four groups, with two or three in the cross section of the tunnel,

The geometrical characteristics of the Acapulco Tunnel are a length of 2,947 m, a cross sectional area of 87.44 $m^2$, with a hydraulic diameter of 9.66 m. The cross section of the tunnel is approximated by a rectangular shape with 7 by 6 cells in the X and Y directions (width versus height), and 159 in the Z direction. The computational domain is therefore divided into 6,678 volume cells. To have a good resolution of the momentum transfer in the near-field of the jet-fans, the grid was made finer therein, and coarser in the tunnel region between the groups of jet-fans.

The Q1 input file is included in the appendix, and there was no modification of the standard ground.f file. Typical relaxation parameters were implemented to obtain convergence with a machine run time of 4 hours 45 minutes.

*Presentation of results*

Overview of cases presented

For the case of cement finished tunnel walls with a surface roughness of 3mm, there was an improved performance for 24 jet-fans over 21, with 3 fans in the cross section as CO concentrations were lower than 100 ppm in the last 500 m of the tunnel, with flow rates of 760 over 719 $m^3$/s. Considering 21 jet-fans there was a small increase of flow rate with 3 fans in the cross section instead of 2, i.e. 719 over 701 $m^3$/s. The flow rate decreased to 687 $m^3$/s for 20 jet-fans, 2 in the cross section.

To have more realistic results, another simulation was effected that considered the momentum source and sink that is due to the vehicle drag in the three tunnel lanes. An increase in wall-roughness was also considered due to tunnel appurtenances such as signs, cable ducts, for which a friction factor of 0.025 was implemented that corresponds to an equivalent wall roughness of 2.5 cm.

In this case the flow rate obtained with 24 jet-fans, 2 in the cross section, was 469 $m^3$/s, a 37% reduction. However, the maximum CO concentration was 148 ppm near ground level at 22 m from the exit portal, which is under the 150 ppm design limit. The momentum sink for the two counterflow lanes was 22.25 kN, while the momentum source for the concurrent lane was 3.2 kN.

Results selected for discussion

The results presented are in a vertical plane along the tunnel length (the Y-Z plane). For the W velocity contours the vertical planes correspond to the location of the jet-fans and the central plane; while for the CO concentration contours, the vertical planes correspond to the three vehicle lanes. It should be noted the vertical scale is amplified 20 times given the length to height aspect ratio of the tunnel.

Figure 1 shows the W-velocity contours where [a] is in the plane of concurrent plane traffic flow, [b] is in the central plane with a countercurrent lane, and [c] is in the plane of the countercurrent lane nearest the tunnel wall. The jet momentum transfer can be appreciated in the upper part of the tunnel, as can be seen in [a] and [c]. Only in certain regions is the average velocity of 5.4 m/s observed. Further, it can be seen that near ground level for the two counterflow lanes, [b] and [c], there is a negative velocity of –6 m/s, which cause recirculation zones at this level and across the tunnel width. In the plane of the counterflow lanes there is a significant vertical velocity gradient in the bottom half of the tunnel, which is absent in the concurrent flow lane, as can be seen in [a]. The momentum source for this lane is 3.2 kN, while the momentum sink for the counterflow lanes is 22.25 kN.

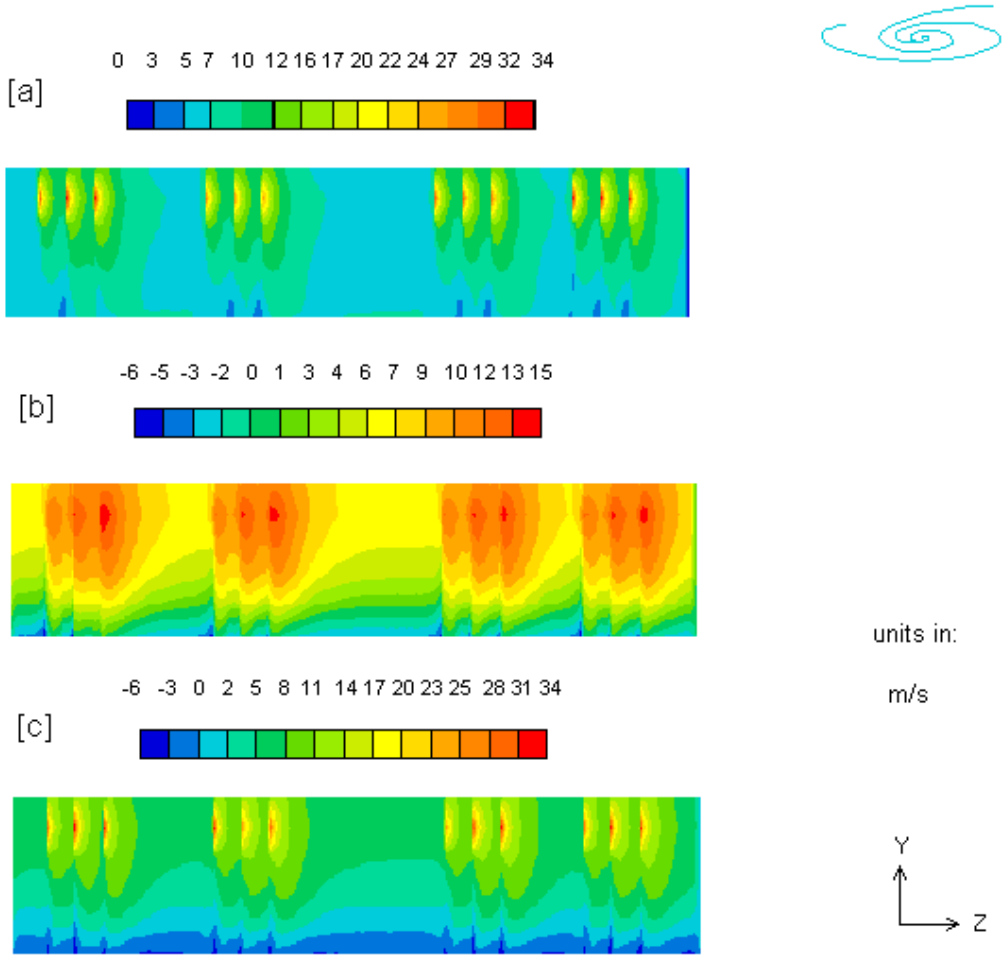


Fig. 1 Tunnel axial velocity contours in the vertical planes of the concurrent traffic flow lane [a], and the two countercurrent traffic flow lanes, [b] and [c]. The jet-fans are in the planes of [a] and [c].

The effect of aerodynamics generated by the jet-fans on the spatial distribution of CO concentration is depicted in Fig. 2, where again ground level vertical gradients are significant, and on the top half of the tunnel they are small. These contours correspond to the same lanes as in Fig. 1, and it is in the concurrent lane that the maximum concentration level of 148 ppm is reached near ground level at a distance 22 m from the exit portal. This is due to the assumption that the two countercurrent lanes entrain fresh air into the tunnel, and therefore the concentration in these two lanes is lower near the exit. It can be appreciated that in the second half of the tunnel, ground level concentrations are higher that 100 ppm, but the section averaged concentrations are lower.

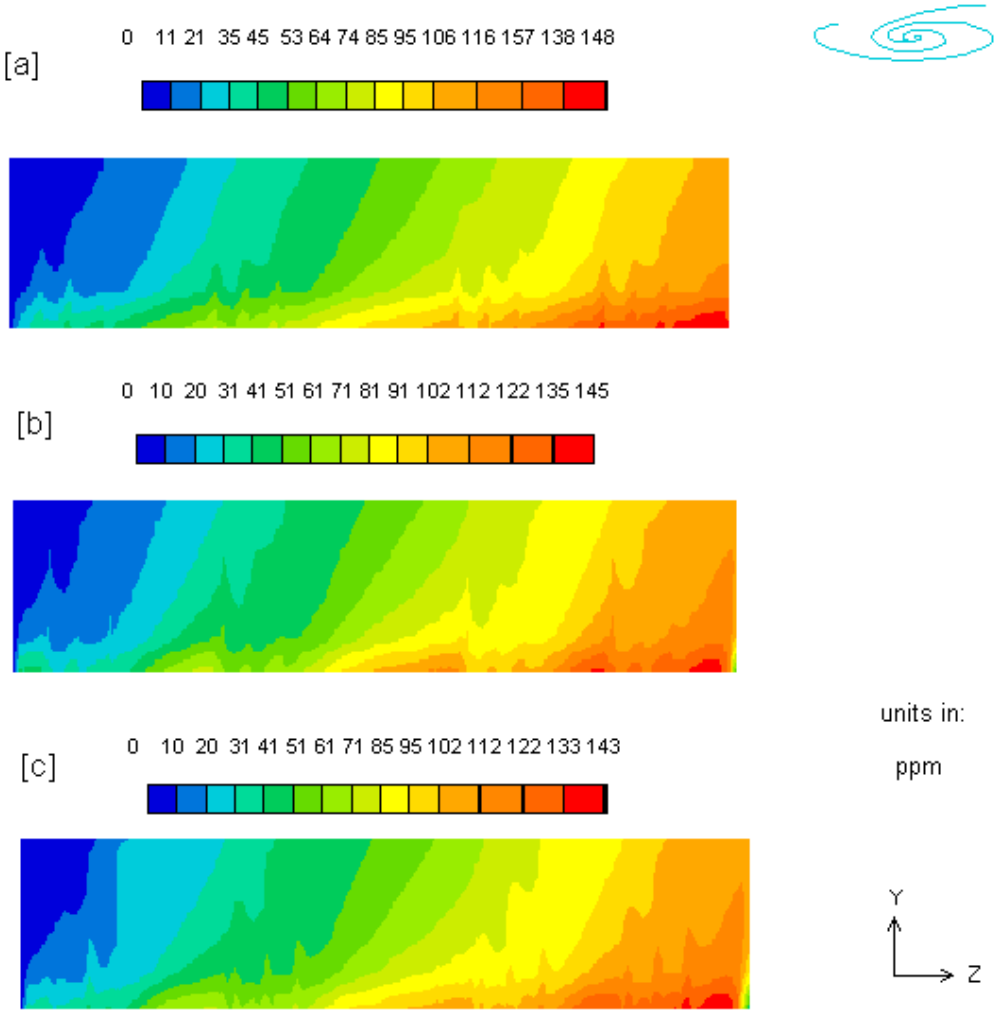


Fig. 2 Tunnel axial CO concentration contours in the same vertical planes as in the previous figure. In the bottom half of the tunnel the concentration gradients are significant in the vertical direction, while in the top half they are in the horizontal direction.

This is observed in Fig. 3 where the CO concentration contours are shown for a transversal plane 22 m form the tunnel exit portal where the highest value was calculated, 148 ppm. Practically 75% of this area has a concentration between 110 and 120 ppm in the upper part of the tunnel. The effect of fresh air entrainment of the two countercurent traffic flow lanes is clearly seen near ground level. These results imply that there is not much transversal mixing between the opposing direction lanes.

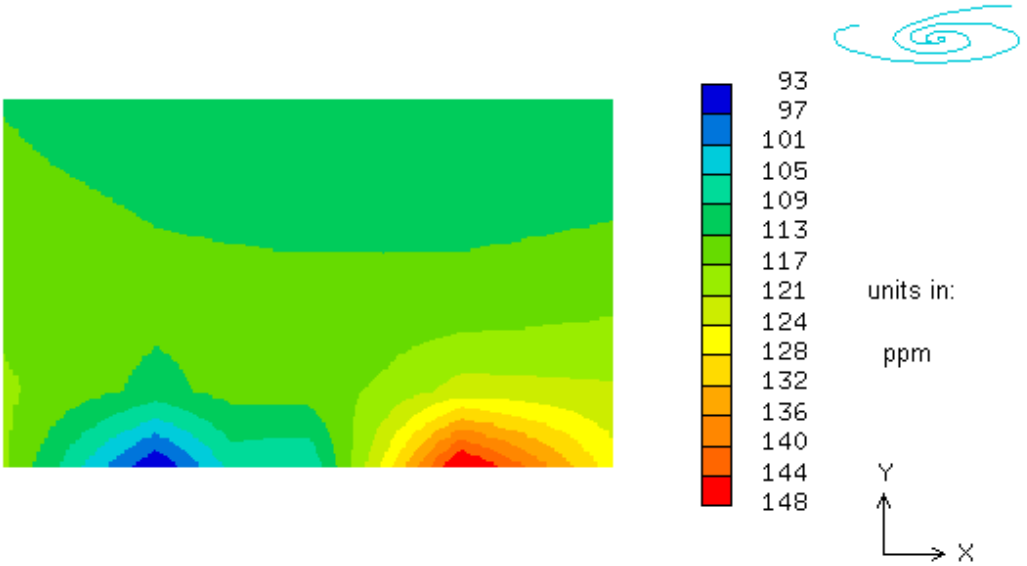


Fig. 3 Carbon dioxide concentration contours in a transversal vertical plane that is located 22 m from the exit portal, where the maximum tunnel concentration was calculated. It is assumed that the two countercurrent traffic flow lanes (depicted on the left side) entrain fresh air from the exit portal.

*Discussion of results*

Except for the last 200 m, the calculations show that the pressure in the tunnel is negative, and the pressure gradient is around 110 Pa/km. In terms of the momentum balance the jet-fan input is consumed in friction (40%) and vehicle drag (60%).

Although there is a good mixing effect by the air jets in the top part of tunnel, there are higher concentration gradients in the bottom half that is caused by the counterflow traffic lanes which considerably affect the axial velocity with recirculation zones.

If the tunnel is unidirectional (i.e. the three lanes are with concurrent traffic flow) then for the same power input there would be a 50 % increase in the flow rate and a 20 % decrease in the maximum CO concentration.

An effect that was not considered in the simulations but that was observed during an inspection of the operating Acapulco Tunnel, was the pressure difference across the tunnel exit and entrance portals that induces an air flow in the tunnel. Thus the portal wind effect tends to abate the CO concentration problem which has required operation of the jet fans only for very congested conditions. The jet-fans are reversible so that the portal pressure difference can always be used to advantage.

The calculations performed consider a CO emission factor of 1 $m^3$/(h.pv) which is a conservative estimate of vehicle emission for the average mexican vehicular park.

*Conclusions and Recommendations*

A fairly straightforward model that calculates the required number of jet-fans for an axially ventilated roadway tunnel has been implemented in PHOENICS. The optimum design can be investigated based on the spatially calculated carbon monoxide concentration distribution.

The overall effect of vehicle drag for countercurrent traffic lanes is considerable; and although it was herein simplified by «moving plates» the results are conservative thus providing a «safety factor» for the maximum ground level CO concentrations allowed.

The calculations derived form an integral approach are based on a very rough estimate of the overall friction factor, and the drag coefficient that is experimentally derived for one vehicle. The overall result would tend to overestimate the required number of jet-fans.

The intermittent nature of vehicle drag effect should be further investigated to have a more realistic mixing effect of the ground level vehicle emissions, and for the fan power requirements for a design airflow rate.

The interaction of the wind on the tunnel portals and traffic-induced airflows should also be further investigated in order to derive worst-case scenarios.

The present model can also be used to investigate a jet-fan operational policy in case of a fire inside the tunnel to ensure maximum safety for trapped vehicle passenger evacuation as well as for fire fighters.

*Literature References*


Baugh, J., W. Ray, F. Black (1987) "Motor vehicle emissions under reduced ambient temperature idle operating conditions." *Atmospheric Environment*, 21 (10), 1045-1058.

Berner, M., J.R. Day (1991). "Alternative methods for ventilating long road tunnels". *Tunnels & Tunnelling* Vol 23 (10) pp. 47-48.

Cory, B., J. Lowndes, R. Matthews (1992). "The aerodynamics of tunnel flows induced by jet fans". *Tunnels & Tunnelling* Vol 24 (10) pp. 31-33.

Gasiorek, J.M. *et al* (1995) Fluid Mechanics 3rd Edition, Longman Scientific and Technical. U.K.

Launder, B.E. y D.B. Spalding (1974) "The Numerical Computation of Turbulent Flow." Comp. Meth in Appl. Mech. and Eng. 3, p. 269.

Ludwig, J.C., Qin, H.Q., and Spalding, D.B. (1990) The PHOENICS Reference Manual for version 1.5, CHAM TR/200, CHAM Ltd, London

Patankar, S.V., and Spalding, D.B. (1972) "A Calculation Procedure for Heat, Mass and Momentum Transfer in Three-dimensional Parabolic Flows", *Int. J. of Heat and Mass Transfer*, Vol. 15, 1787-1806

Péra, J. (1989). "The design of long road tunnels: an overview" *Tunnels & Tunnelling* Vol 21 (1) pp. 17-19.

Túnel Acapulco - Cálculo de la Ventilación (1995). Informe de ICA I**NGENIERÍA**, febrero-mayo.

## *Appendix*

### Q1 input file

```
TALK=f;RUN( 1, 1);VDU=X11-TERM
 IRUNN   =       1 ;LIBREF =       0
 ************************************************************
  Group 1. Run Title
 TEXT( 24 Jet-fans, 2 in section; 2 lanes <----)
 ************************************************************
  Group 2. Transience
 STEADY  =    T
 ************************************************************
  Groups 3, 4, 5  Grid Information
    * Overall number of cells, RSET(M,NX,NY,NZ,tolerance)
 RSET(M,7,6,159)
    * Set overall domain extent:
    *        xulast  yvlast  zwlast    name
 XSI= 1.220E+01;YSI= 7.176E+00;ZSI= 2.947E+03;RSET(D,TUNEL   )
    * Set objects: x0     y0     z0
    *              dx     dy     dz    name
 XPO= 3.328E+00;YPO= 4.866E+00;ZPO= 1.500E+02
 XSI= 1.108E+00;YSI= 1.104E+00;ZSI= 4.000E+00;RSET(B,FN11    )
 XPO= 5.546E+00;YPO= 4.866E+00;ZPO= 1.500E+02
 XSI= 1.108E+00;YSI= 1.104E+00;ZSI= 4.000E+00;RSET(B,FN12    )
 XPO= 7.764E+00;YPO= 4.866E+00;ZPO= 1.500E+02
 XSI= 1.108E+00;YSI= 1.104E+00;ZSI= 4.000E+00;RSET(B,FN13    )
 XPO= 7.764E+00;YPO= 4.866E+00;ZPO= 2.700E+02
 XSI= 1.108E+00;YSI= 1.104E+00;ZSI= 4.000E+00;RSET(B,FN23    )
 XPO= 5.546E+00;YPO= 4.866E+00;ZPO= 2.700E+02
 XSI= 1.108E+00;YSI= 1.104E+00;ZSI= 4.000E+00;RSET(B,FN22    )
 XPO= 3.328E+00;YPO= 4.866E+00;ZPO= 2.700E+02
 XSI= 1.108E+00;YSI= 1.104E+00;ZSI= 4.000E+00;RSET(B,FN21    )
 XPO= 3.328E+00;YPO= 4.866E+00;ZPO= 3.900E+02
 XSI= 1.108E+00;YSI= 1.104E+00;ZSI= 4.000E+00;RSET(B,FN31    )
 XPO= 5.546E+00;YPO= 4.866E+00;ZPO= 3.900E+02
 XSI= 1.108E+00;YSI= 1.104E+00;ZSI= 4.000E+00;RSET(B,FN32    )
 XPO= 7.764E+00;YPO= 4.866E+00;ZPO= 3.900E+02
 XSI= 1.108E+00;YSI= 1.104E+00;ZSI= 4.000E+00;RSET(B,FN33    )
 XPO= 3.328E+00;YPO= 4.866E+00;ZPO= 8.630E+02
 XSI= 1.108E+00;YSI= 1.104E+00;ZSI= 4.000E+00;RSET(B,B10     )
 XPO= 5.546E+00;YPO= 4.866E+00;ZPO= 8.630E+02
 XSI= 1.108E+00;YSI= 1.104E+00;ZSI= 4.000E+00;RSET(B,B11     )
 XPO= 7.764E+00;YPO= 4.866E+00;ZPO= 8.630E+02
 XSI= 1.108E+00;YSI= 1.104E+00;ZSI= 4.000E+00;RSET(B,B12     )
 XPO= 3.328E+00;YPO= 4.866E+00;ZPO= 9.830E+02
 XSI= 1.108E+00;YSI= 1.104E+00;ZSI= 4.000E+00;RSET(B,B13     )
 XPO= 5.546E+00;YPO= 4.866E+00;ZPO= 9.830E+02
 XSI= 1.108E+00;YSI= 1.104E+00;ZSI= 4.000E+00;RSET(B,B14     )
 XPO= 7.764E+00;YPO= 4.866E+00;ZPO= 9.830E+02
 XSI= 1.108E+00;YSI= 1.104E+00;ZSI= 4.000E+00;RSET(B,B15     )
 XPO= 3.328E+00;YPO= 4.866E+00;ZPO= 1.103E+03
 XSI= 1.108E+00;YSI= 1.104E+00;ZSI= 4.000E+00;RSET(B,B16     )
 XPO= 5.546E+00;YPO= 4.866E+00;ZPO= 1.103E+03
 XSI= 1.108E+00;YSI= 1.104E+00;ZSI= 4.000E+00;RSET(B,B17     )
 XPO= 7.764E+00;YPO= 4.866E+00;ZPO= 1.103E+03
 XSI= 1.108E+00;YSI= 1.104E+00;ZSI= 4.000E+00;RSET(B,B18     )
 XPO= 3.328E+00;YPO= 4.866E+00;ZPO= 1.844E+03
```

```
XSI= 1.108E+00;YSI= 1.104E+00;ZSI= 4.000E+00;RSET(B,B19     )
XPO= 5.546E+00;YPO= 4.866E+00;ZPO= 1.844E+03
XSI= 1.108E+00;YSI= 1.104E+00;ZSI= 4.000E+00;RSET(B,B20     )
XPO= 7.764E+00;YPO= 4.866E+00;ZPO= 1.844E+03
XSI= 1.108E+00;YSI= 1.104E+00;ZSI= 4.000E+00;RSET(B,B21     )
XPO= 3.328E+00;YPO= 4.866E+00;ZPO= 1.964E+03
XSI= 1.108E+00;YSI= 1.104E+00;ZSI= 4.000E+00;RSET(B,B22     )
XPO= 5.546E+00;YPO= 4.866E+00;ZPO= 1.964E+03
XSI= 1.108E+00;YSI= 1.104E+00;ZSI= 4.000E+00;RSET(B,B23     )
XPO= 7.764E+00;YPO= 4.866E+00;ZPO= 1.964E+03
XSI= 1.108E+00;YSI= 1.104E+00;ZSI= 4.000E+00;RSET(B,B24     )
XPO= 3.328E+00;YPO= 4.866E+00;ZPO= 2.084E+03
XSI= 1.108E+00;YSI= 1.104E+00;ZSI= 4.000E+00;RSET(B,B25     )
XPO= 5.546E+00;YPO= 4.866E+00;ZPO= 2.084E+03
XSI= 1.108E+00;YSI= 1.104E+00;ZSI= 4.000E+00;RSET(B,B26     )
XPO= 7.764E+00;YPO= 4.866E+00;ZPO= 2.084E+03
XSI= 1.108E+00;YSI= 1.104E+00;ZSI= 4.000E+00;RSET(B,B27     )
XPO= 3.328E+00;YPO= 4.866E+00;ZPO= 2.437E+03
XSI= 1.108E+00;YSI= 1.104E+00;ZSI= 4.000E+00;RSET(B,B28     )
XPO= 7.764E+00;YPO= 4.866E+00;ZPO= 2.437E+03
XSI= 1.108E+00;YSI= 1.104E+00;ZSI= 4.000E+00;RSET(B,B29     )
XPO= 5.546E+00;YPO= 4.866E+00;ZPO= 2.437E+03
XSI= 1.108E+00;YSI= 1.104E+00;ZSI= 4.000E+00;RSET(B,B30     )
XPO= 3.328E+00;YPO= 4.866E+00;ZPO= 2.557E+03
XSI= 1.108E+00;YSI= 1.104E+00;ZSI= 4.000E+00;RSET(B,B31     )
XPO= 5.546E+00;YPO= 4.866E+00;ZPO= 2.557E+03
XSI= 1.108E+00;YSI= 1.104E+00;ZSI= 4.000E+00;RSET(B,B32     )
XPO= 7.764E+00;YPO= 4.866E+00;ZPO= 2.557E+03
XSI= 1.108E+00;YSI= 1.104E+00;ZSI= 4.000E+00;RSET(B,B33     )
XPO= 3.328E+00;YPO= 4.866E+00;ZPO= 2.677E+03
XSI= 1.108E+00;YSI= 1.104E+00;ZSI= 4.000E+00;RSET(B,B34     )
XPO= 5.546E+00;YPO= 4.866E+00;ZPO= 2.677E+03
XSI= 1.108E+00;YSI= 1.104E+00;ZSI= 4.000E+00;RSET(B,B35     )
XPO= 7.764E+00;YPO= 4.866E+00;ZPO= 2.677E+03
XSI= 1.108E+00;YSI= 1.104E+00;ZSI= 4.000E+00;RSET(B,B36     )
XPO=  .000E+00;YPO=  .000E+00;ZPO=  .000E+00
XSI= 1.220E+01;YSI=  .000E+00;ZSI= 2.947E+03;RSET(B,PISO    )
XPO=  .000E+00;YPO= 7.176E+00;ZPO=  .000E+00
XSI= 1.220E+01;YSI=  .000E+00;ZSI= 2.947E+03;RSET(B,TECHO   )
XPO= 1.220E+01;YPO=  .000E+00;ZPO=  .000E+00
XSI=  .000E+00;YSI= 7.176E+00;ZSI= 2.947E+03;RSET(B,PRD1    )
XPO=  .000E+00;YPO=  .000E+00;ZPO=  .000E+00
XSI=  .000E+00;YSI= 7.176E+00;ZSI= 2.947E+03;RSET(B,PRD2    )
XPO=  .000E+00;YPO=  .000E+00;ZPO= 2.088E+03
XSI= 1.220E+01;YSI= 7.176E+00;ZSI= 3.490E+02;RSET(B,B41     )
RSET(Z,1,7,1.000E+00)
RSET(Z,2,2,1.000E+00)
RSET(Z,3,5,1.000E+00)
RSET(Z,4,2,1.000E+00)
RSET(Z,5,5,1.000E+00)
RSET(Z,6,2,1.000E+00)
RSET(Z,7,22,1.000E+00)
RSET(Z,8,2,1.000E+00)
RSET(Z,9,5,1.000E+00)
RSET(Z,10,2,1.000E+00)
RSET(Z,11,5,1.000E+00)
RSET(Z,12,2,1.000E+00)
RSET(Z,13,37,1.000E+00)
RSET(Z,14,2,1.000E+00)
RSET(Z,15,5,1.000E+00)
RSET(Z,16,2,1.000E+00)
RSET(Z,17,5,1.000E+00)
RSET(Z,18,2,1.000E+00)
RSET(Z,19,17,1.000E+00)
RSET(Z,20,2,1.000E+00)
RSET(Z,21,5,1.000E+00)
RSET(Z,22,2,1.000E+00)
RSET(Z,23,5,1.000E+00)
RSET(Z,24,2,1.000E+00)
RSET(Z,25,12,1.000E+00)
************************************************************
 Group 6. Body-Fitted coordinates
************************************************************
 Group 7. Variables: STOREd,SOLVEd,NAMEd
```

```
ONEPHS  =    T
   * Non-default variable names
NAME(47) =NPOR ; NAME(48) =PPM
NAME(49) =DEN1 ; NAME(50) =ENUT
   * Solved variables list
SOLVE(P1  ,U1  ,V1  ,W1  ,KE  ,EP  ,PPM )
   * Stored variables list
STORE(ENUT,DEN1,NPOR)
   * Additional solver options
SOLUTN(P1  ,Y,Y,Y,N,N,Y)
SOLUTN(KE  ,Y,Y,N,N,N,N)
SOLUTN(EP  ,Y,Y,N,N,N,N)
************************************************************
 Group 8. Terms & Devices
TERMS (KE  ,N,Y,Y,Y,Y,N)
TERMS (EP  ,N,Y,Y,Y,Y,N)
NEWENT  =    T
************************************************************
 Group 9. Properties
RHO1    = 1.189E+00
EL1     = GRND4
ENUL    = 1.544E-05 ;ENUT   = GRND3
PRT   (EP  ) =  1.314E+00
************************************************************
 Group 10.Inter-Phase Transfer Processes
************************************************************
 Group 11.Initialise Var/Porosity Fields
FIINIT(KE  ) =  2.000E-04 ;FIINIT(EP  ) =  2.332E-05
FIINIT(NPOR) =  1.000E+00
  No PATCHes used for this Group

RSTGRD  =    F

INIADD  =    F
************************************************************
 Group 12. Convection and diffusion adjustments
************************************************************
 Group 13. Boundary & Special Sources

PATCH (KESOURCE,PHASEM,1,7,1,6,1,159,1,1)
COVAL (KESOURCE,KE  , GRND4    , GRND4    )
COVAL (KESOURCE,EP  , GRND4    , GRND4    )

PATCH (PISO    ,SWALL ,#1,#7,#1,#1,#1,#25,1,1)
COVAL (PISO    ,U1  , GRND2    ,  .000E+00)
COVAL (PISO    ,W1  , GRND2    ,  .000E+00)
COVAL (PISO    ,KE  , GRND2    , GRND2    )
COVAL (PISO    ,EP  , GRND2    , GRND2    )

PATCH (CARRIL1 ,SWALL , 2, 2, 2, 2, 1,159,1,1)
COVAL (CARRIL1 ,W1  , GRND2    ,-13.88E+00)
COVAL (CARRIL1 ,KE  , GRND2    , GRND2    )
COVAL (CARRIL1 ,EP  , GRND2    , GRND2    )

PATCH (CARRIL2 ,SWALL , 4, 4, 2, 2, 1,159,1,1)
COVAL (CARRIL2 ,W1  , GRND2    ,-13.88E+00)
COVAL (CARRIL2 ,KE  , GRND2    , GRND2    )
COVAL (CARRIL2 ,EP  , GRND2    , GRND2    )

PATCH (CARRIL3 ,SWALL , 6, 6, 2, 2, 1,159,1,1)
COVAL (CARRIL3 ,W1  , GRND2    , 13.88E+00)
COVAL (CARRIL3 ,KE  , GRND2    , GRND2    )
COVAL (CARRIL3 ,EP  , GRND2    , GRND2    )

PATCH (CARRIL1a,nWALL , 2, 2, 1, 1, 1,159,1,1)
COVAL (CARRIL1a,W1  , GRND2    ,-13.88E+00)
COVAL (CARRIL1a,KE  , GRND2    , GRND2    )
COVAL (CARRIL1a,EP  , GRND2    , GRND2    )

PATCH (CARRIL2a,nWALL , 4, 4, 1, 1, 1,159,1,1)
COVAL (CARRIL2a,W1  , GRND2    ,-13.88E+00)
COVAL (CARRIL2a,KE  , GRND2    , GRND2    )
COVAL (CARRIL2a,EP  , GRND2    , GRND2    )
```

```
PATCH (CARRIL3a,nWALL , 6, 6, 1, 1, 1,159,1,1)
COVAL (CARRIL3a,W1  , GRND2    , 13.88E+00)
COVAL (CARRIL3a,KE  , GRND2    , GRND2    )
COVAL (CARRIL3a,EP  , GRND2    , GRND2    )

PATCH (CARRoL1a,eWALL , 2, 2, 1, 1, 1,159,1,1)
COVAL (CARRoL1a,W1  , GRND2    ,-13.88E+00)
COVAL (CARRoL1a,KE  , GRND2    , GRND2    )
COVAL (CARRoL1a,EP  , GRND2    , GRND2    )

PATCH (CARRoL2a,eWALL , 4, 4, 1, 1, 1,159,1,1)
COVAL (CARRoL2a,W1  , GRND2    ,-13.88E+00)
COVAL (CARRoL2a,KE  , GRND2    , GRND2    )
COVAL (CARRoL2a,EP  , GRND2    , GRND2    )

PATCH (CARRoL3a,eWALL , 6, 6, 1, 1, 1,159,1,1)
COVAL (CARRoL3a,W1  , GRND2    , 13.88E+00)
COVAL (CARRoL3a,KE  , GRND2    , GRND2    )
COVAL (CARRoL3a,EP  , GRND2    , GRND2    )

PATCH (CARRoL1b,wWALL , 2, 2, 1, 1, 1,159,1,1)
COVAL (CARRoL1b,W1  , GRND2    ,-13.88E+00)
COVAL (CARRoL1b,KE  , GRND2    , GRND2    )
COVAL (CARRoL1b,EP  , GRND2    , GRND2    )

PATCH (CARRoL2b,wWALL , 4, 4, 1, 1, 1,159,1,1)
COVAL (CARRoL2b,W1  , GRND2    ,-13.88E+00)
COVAL (CARRoL2b,KE  , GRND2    , GRND2    )
COVAL (CARRoL2b,EP  , GRND2    , GRND2    )

PATCH (CARRoL3b,wWALL , 6, 6, 1, 1, 1,159,1,1)
COVAL (CARRoL3b,W1  , GRND2    , 13.88E+00)
COVAL (CARRoL3b,KE  , GRND2    , GRND2    )
COVAL (CARRoL3b,EP  , GRND2    , GRND2    )

PATCH (TECHO   ,NWALL ,#1,#7,#3,#3,#1,#25,1,1)
PATCH (TECHO   ,NWALL ,#1,#7,#3,#3,#1,#25,1,1)
COVAL (TECHO   ,U1  , GRND2    ,  .000E+00)
COVAL (TECHO   ,W1  , GRND2    ,  .000E+00)
COVAL (TECHO   ,KE  , GRND2    , GRND2    )
COVAL (TECHO   ,EP  , GRND2    , GRND2    )

PATCH (PRD1    ,EWALL ,#7,#7,#1,#3,#1,#25,1,1)
COVAL (PRD1    ,V1  , GRND2    ,  .000E+00)
COVAL (PRD1    ,W1  , GRND2    ,  .000E+00)
COVAL (PRD1    ,KE  , GRND2    , GRND2    )
COVAL (PRD1    ,EP  , GRND2    , GRND2    )

PATCH (PRD2    ,WWALL ,#1,#1,#1,#3,#1,#25,1,1)
COVAL (PRD2    ,V1  , GRND2    ,  .000E+00)
COVAL (PRD2    ,W1  , GRND2    ,  .000E+00)
COVAL (PRD2    ,KE  , GRND2    , GRND2    )
COVAL (PRD2    ,EP  , GRND2    , GRND2    )

PATCH (MEX     ,LOW   ,#1,#7,#1,#3,#1,#1,1,1)
COVAL (MEX     ,P1  , 1.000E+00,  .000E+00)
COVAL (MEX     ,KE  ,  .000E+00, SAME     )
COVAL (MEX     ,EP  ,  .000E+00, SAME     )

PATCH (ACA     ,HIGH  ,#1,#7,#1,#3,#25,#25,1,1)
COVAL (ACA     ,P1  , FIXVAL   ,  .000E+00)
COVAL (ACA     ,KE  ,  .000E+00, SAME     )
COVAL (ACA     ,EP  ,  .000E+00, SAME     )
     COVAL (ACA     ,PPM ,  .000E+00, SAME     )
COVAL (ACA     ,PPM ,  .000E+00, 0.00E+00)

PATCH (FN01    ,HIGH  ,2,2,5,5,9,9,1,1)
COVAL (FN01    ,W1  , FIXVAL   , 3.400E+01)

PATCH (FN02    ,HIGH  ,2,2,5,5,16,16,1,1)
COVAL (FN02    ,W1  , FIXVAL   , 3.400E+01)

PATCH (FN03    ,HIGH  ,2,2,5,5,23,23,1,1)
COVAL (FN03    ,W1  , FIXVAL   , 3.400E+01)
```

```
PATCH (FN04    ,HIGH  ,2,2,5,5,47,47,1,1)
COVAL (FN04    ,W1  , FIXVAL   , 3.400E+01)

PATCH (FN05    ,HIGH  ,2,2,5,5,54,54,1,1)
COVAL (FN05    ,W1  , FIXVAL   , 3.400E+01)

PATCH (FN06    ,HIGH  ,2,2,5,5,61,61,1,1)
COVAL (FN06    ,W1  , FIXVAL   , 3.400E+01)

PATCH (FN07    ,HIGH  ,2,2,5,5,100,100,1,1)
COVAL (FN07    ,W1  , FIXVAL   , 3.400E+01)

PATCH (FN08    ,HIGH  ,2,2,5,5,107,107,1,1)
COVAL (FN08    ,W1  , FIXVAL   , 3.400E+01)

PATCH (FN09    ,HIGH  ,2,2,5,5,114,114,1,1)
COVAL (FN09    ,W1  , FIXVAL   , 3.400E+01)

PATCH (FN10    ,HIGH  ,2,2,5,5,133,133,1,1)
COVAL (FN10    ,W1  , FIXVAL   , 3.400E+01)

PATCH (FN11    ,HIGH  ,2,2,5,5,140,140,1,1)
COVAL (FN11    ,W1  , FIXVAL   , 3.400E+01)

PATCH (FN12    ,HIGH  ,2,2,5,5,147,147,1,1)
COVAL (FN12    ,W1  , FIXVAL   , 3.400E+01)

PATCH (FB01    ,HIGH  ,6,6,5,5,9,9,1,1)
COVAL (FB01    ,W1  , FIXVAL   , 3.400E+01)

PATCH (FB02    ,HIGH  ,6,6,5,5,16,16,1,1)
COVAL (FB02    ,W1  , FIXVAL   , 3.400E+01)

PATCH (FB03    ,HIGH  ,6,6,5,5,23,23,1,1)
COVAL (FB03    ,W1  , FIXVAL   , 3.400E+01)

PATCH (FB04    ,HIGH  ,6,6,5,5,47,47,1,1)
COVAL (FB04    ,W1  , FIXVAL   , 3.400E+01)

PATCH (FB05    ,HIGH  ,6,6,5,5,54,54,1,1)
COVAL (FB05    ,W1  , FIXVAL   , 3.400E+01)

PATCH (FB06    ,HIGH  ,6,6,5,5,61,61,1,1)
COVAL (FB06    ,W1  , FIXVAL   , 3.400E+01)

PATCH (FB07    ,HIGH  ,6,6,5,5,100,100,1,1)
COVAL (FB07    ,W1  , FIXVAL   , 3.400E+01)

PATCH (FB08    ,HIGH  ,6,6,5,5,107,107,1,1)
COVAL (FB08    ,W1  , FIXVAL   , 3.400E+01)

PATCH (FB09    ,HIGH  ,6,6,5,5,114,114,1,1)
COVAL (FB09    ,W1  , FIXVAL   , 3.400E+01)

PATCH (FB10    ,HIGH  ,6,6,5,5,133,133,1,1)
COVAL (FB10    ,W1  , FIXVAL   , 3.400E+01)

PATCH (FB11    ,HIGH  ,6,6,5,5,140,140,1,1)
COVAL (FB11    ,W1  , FIXVAL   , 3.400E+01)

PATCH (FB12    ,HIGH  ,6,6,5,5,147,147,1,1)
COVAL (FB12    ,W1  , FIXVAL   , 3.400E+01)

PATCH (CCC1    ,VOLUME,2,2,1,1,1,159,1,1)
COVAL (CCC1    ,PPM , FIXFLU   , 5.500E+00)

PATCH (CCC2    ,VOLUME,6,6,1,1,1,159,1,1)
COVAL (CCC2    ,PPM , FIXFLU   , 5.500E+00)

PATCH (CCC3    ,VOLUME,4,4,1,1,1,159,1,1)
COVAL (CCC3    ,PPM , FIXFLU   , 5.500E+00)

WALLA   = 2.500E-02 ;WALLB  =  .000E+00
```

```
 ************************************************************
  Group 14. Downstream Pressure For PARAB
 ************************************************************
  Group 15. Terminate Sweeps
 LSWEEP  =  5000
restrt(all)
 SELREF  =    F
 RESFAC  = 1.000E-02
 ************************************************************
  Group 16. Terminate Iterations
 ENDIT (P1  ) =  1.000E-03 ;ENDIT (U1  ) =  1.000E-03
 ENDIT (V1  ) =  1.000E-03 ;ENDIT (W1  ) =  1.000E-03
 ENDIT (KE  ) =  1.000E-03 ;ENDIT (EP  ) =  1.000E-03
 ENDIT (PPM ) =  1.000E-03
 ************************************************************
  Group 17. Relaxation
 RELAX(P1  ,LINRLX, 1.000E+00)
 RELAX(KE  ,FALSDT, 1.500E+00)
 RELAX(EP  ,FALSDT, 1.500E+00)
 RELAX(PPM ,FALSDT, 1.500E+02)
 KELIN   =       0
 ************************************************************
  Group 18. Limits
 ************************************************************
  Group 19. EARTH Calls To GROUND Station
 GENK    =    T
 ************************************************************
  Group 20. Preliminary Printout
 ECHO    =    T
 ************************************************************
  Group 21. Print-out of Variables
 ************************************************************
  Group 22. Monitor Print-Out
 IXMON   = 4 ;IYMON  = 3 ;IZMON  =  13
 TSTSWP  = -5
 ************************************************************
  Group 23.Field Print-Out & Plot Control
 ITABL   =       1
   No PATCHes used for this Group
 ************************************************************
  Group 24. Dumps For Restarts
 ************************************************************
 MENSAV(S,RELX,DEF,1.1960E+00,1.0000E-05,0)
 MENSAV(S,PHSPROP,DEF,200,0,1.1890E+00,1.5440E-05)
 MENSAV(S,FLPRP,DEF,K-E,CONSTANT)
STOP
```